RSC Advances

ROYAL SOCIETY OF CHEMISTRY

www.rsc.org/advances

RSC Advances

COMMUNICATION

Improved efficiency and stability of organic photovoltaic device using UV-ozone treated ZnO anode buffer

Received 28th July 2015,
Accepted 00th January 20xx

DOI: 10.1039/x0xx00000x

www.rsc.org/

Chiu-Yee Chan [a], Yu-Fang Wei [a], Hrisheekesh Thachoth Chandran [a], Chun-Sing Lee [a, b], Ming-Fai Lo [a, b*] and Tsz-Wai Ng [a, b *]

The efficiency of boron subphthalocyanine chloride/ fullerene device is enhanced from 2.5% to 3.2 % after inserting an UV ozone treated ZnO (UV-ZnO) which is due to improved SubPc absorption by light scattering. Moreover, UV-ZnO device shows < 5 % PCE drop while standard device shows 35% drop because of the stable high work function of UV-ZnO layer.

Organic photovoltaic (OPV) devices have attracted much interest because of their flexibilities, low cost, and ease in device fabrication [1]. Although there are continuous improvements in reported power conversion efficiencies (PCE), the device operation stability and reliability are still major hurdles for wide applications. There are several reports on the degradation mechanism of the OPV devices. Environmental conditions including light, oxygen and moisture [2] are shown to be major factors that damage the chemical structure [3-5] and affect the charge transport [6], and light absorption [7-9] of organic films.

Even with good encapsulation techniques, obvious devices degradation can still be observed after timed operation. While most studies attribute such device degradation to gradual decrease of indium tin oxide (ITO) work function [10, 11], our group has recently found out that the common ultraviolet (UV) ozone plasma treatment of ITO substrate has detrimental effect to chemical and electronic properties of the addlayer organic films [12]. Apart from UV ozone treatment, other plasma post treatment using chlorine [13] fluorocarbon [14, 15] gases, etc. have been employed for ITO substrates.

Another simple approach is to insert an anode buffer layer, such as graphene oxide [16-18], poly(3, 4-ethylenedioxythiophene): poly(styrenesulfonate) (PEDOT: PSS) [19], vanadium pentoxide (V_2O_5) [20], molybdenum trioxide (MoO_3) [21], nickel oxide (NiO_x) [22, 23], copper oxide (CuO_x)[24], ruthenium oxide (RuO_x)[25] and rhenium oxide(ReO_x)[26]. Among all these buffer materials, PEDOT: PSS [27] and MoO_3 [28-30] with high work functions of 5.2 and 6.9 eV respectively are commonly used due to their hole extracting abilities towards ITO anode. However, these materials are chemically unstable. For example, PEDOT: PSS is acidic in nature, which can corrode both the ITO substrate [31, 32] and top organic films [10]. Also, the work function can be significantly reduced when the MoO_3 is non-stoichiometric. [33 34]

In this work, we show that zinc oxide (ZnO) film prepared by simple solution process can be an alternate candidate for anode buffer layer. Although the work function of ZnO is small (4.5 eV) [35, 36], it can be dramatically enhanced to 5.1 eV by UV ozone plasma treatment. Most importantly, the UV ozone treated ZnO is much stable compared to ITO substrate. OPV device with UV ozone treated ZnO buffer can show 28 % improvement in PCE from 2.5% to 3.2 %. Meanwhile, only less than 5 % drop in PCE is observed in this device under continuous illumination for 60 minutes.

ITO-coated glasses with a sheet resistance of 30 Ω/ square were routinely cleaned and dried in an oven, and finally treated in

[a] Centre of Super-Diamond and Advanced Films (COSDAF), Department of Physics and Materials Science, City University of Hong Kong, Hong Kong SAR, P. R. China E mail: tszwaing@cityu.edu.hk (Tsz-Wai Ng), mingflo@ cityu.edu.hk (Ming-Fai Lo)
[b] City University of Hong Kong Shenzhen Research Institute, Shenzhen, People's Republic of China.

UV ozone chamber for 15 minutes. To prepare the ZnO buffer layer, the cleaned ITO substrates were dipped in to $5x10^{-3}$ M zinc acetate ethanol solution for 3, 5, 7 and 10 minutes respectively. The samples were annealed at a temperature of 200˚C for 20 minutes and cooled in furnace. The thickness of ZnO coating was characterized using scanning electron microscope using Philips XL 30 FEG with results shown in table 1. The surface roughness is measured by atomic force microscope (Nanoscope IIIa).

Devices were fabricated with structure of: substrates/ SubPc (17 nm)/ C_{60} (40 nm)/ Bphen (10 nm)/ Al (80nm). The substrates used include ITO, ITO/ZnO with or without post UV ozone treatment. All the organic films were prepared by thermal evaporation under 10^{-5} Pa with a controlled rate of 1 Å s^{-1}. These organic materials (i.e. SubPc, C_{60} and Bphen) from Luminescence Technology Corporation were used as received. Following the deposition of organic films, Al cathode was deposited with a shadow mask with defined active device area of 0.1 cm^2. Devices were encapsulated immediately in glove box after the fabrication. The current density-voltage (J-V) characteristics of the devices were measured by a programmable Keithley model 237 power source under AM 1.5G illumination at 100 mW cm^{-2} from a Newport Oriel Solar Simulator. Photoelectron studies were carried out with a VG ESCALAB 220i-XL surface analysis system equipped with a He-discharge lamp providing He-I photons of 21.22 eV for UPS analysis [37].

OPV devices with a structure of substrate / SubPc (17nm)/ C_{60} (40nm)/ Bphen (10nm)/ Al (80nm) are fabricated on an ITO substrate **(UV-ITO device)**, ITO/ZnO substrates with (**UV-ZnO device)** and without **(non-UV-ZnO device)** post UV ozone treatment. Fig.1a shows the J-V characteristics of the optimized **UV-ITO device**, **non UV-ZnO device** and **UV-ZnO device** under 1 sun illumination. The **UV-ITO standard device** shows an open circuit voltage (Voc), a short circuit current density (Jsc), a fill factor (FF) and a PCE of 0.9 V, 5.0 mA/cm^2, 0.52 and 2.5 % respectively (black line). Table 1 shows that the **UV-ZnO device** performance varies with the thickness of ZnO layer. The device has an optimized performance at a thickness of 100 nm and exhibits a good performance with a Voc, Jsc, FF, PCE of 1.06 V, 5.9 mA/cm^2m, 0.52 and 3.2% respectively (blue line). For a fair comparison, a **non-UV-ZnO device** with the same thickness of ZnO (100 nm) is also fabricated. Yet, it shows a poor performance with the Voc, Jsc, FF and PCE of 0.14 V, 3.7 mA/cm^2, 0.33 and 0.17%, respectively (red line). The PCE of the **UV-ZnO device** is greatly enhanced from 0.17% to 3.2% when compares with the non-UV-ZnO device. It is worth noting that the **UV-ZnO device** has PCE 28 % higher than **UV-ITO device**.

Table 1 Device performance parameters of the standard device and UV-ZnO devices.

ZnO thickness/ nm	Jsc/ mAcm^{-2}	Voc/ V	FF	PCE/ %
0 (standard)	**5.0**	**0.90**	**0.52**	**2.5**
80	**4.0**	**1.00**	**0.39**	**1.6**
90	**5.1**	**1.03**	**0.42**	**2.2**
100	**5.9**	**1.06**	**0.52**	**3.2**
120	**4.3**	**0.90**	**0.39**	**1.5**

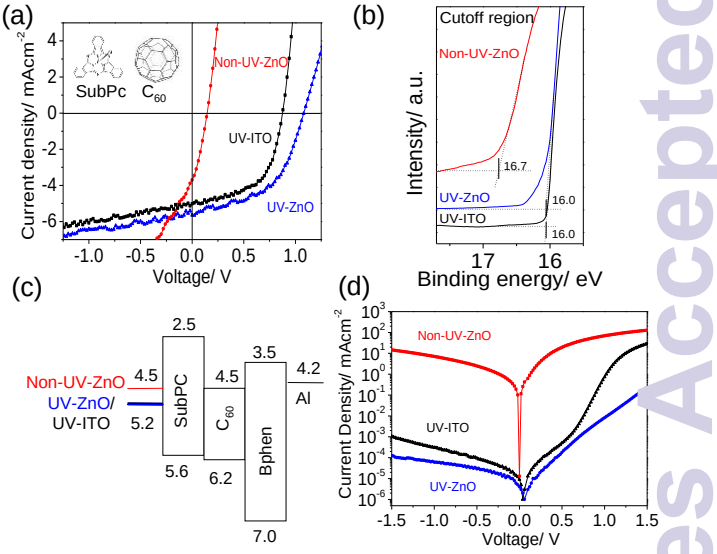

Fig 1. (a) Photocurrent density-voltage (J-V) curves of the standard UV-ITO, UV-ZnO and non-UV-ZnO devices under 100 mWcm^{-2} illumination. Device structure is: ITO/ ZnO (100nm)/ SubPc(17nm)/ C_{60} (40nm)/ Bphen (10nm)/ Al (80nm). Inset is the chemical structure of SubPc and C_{60}. (b) UPS spectra of the standard UV-ITO, and ITO/ ZnO(100nm) substrates with and without UV-ozone treatment (c) Schematic band diagram of SubPc-C_{60} devices on ITO, non-UV-ZnO and UV-ZnO substrates. (d) The dark J-V curve of the corresponding devices.

In order to probe the role of post UV ozone treatment to device performance, we examine the electronic structure of these substrates using UPS studies. Fig. 1b shows the cutoff region of the UPS spectra of ITO/ZnO with **(UV-ZnO sample)** or without **(non-UV**

ZnO sample) post UV ozone treatment. A reference **UV-ITO sample** is also shown. For **non-UV-ZnO sample**, the cutoff region is at 16.7 eV, which is corresponds to a work function of 4.5 eV. After the post UV ozone treatment, the **UV-ZnO sample** has a spectral cutoff positioned at 16.0 eV. This value is similar to that of the **UV-ITO sample**, showing a work function of 5.2 eV. Fig. 1c shows the schematic energy level diagram of the SubPc/C_{60} based devices with different anode substrates.

In Fig. 1c, the **non-UV-ZnO sample** has a low work function of 4.5 eV similar to that of the Al cathode (4.2 eV). The work function difference between two electrodes is small which results in a limited built-in field in the device. After exciton dissociation, the free holes and electrons would readily recombine before they are extracted to the electrodes. This can be reflected by the large shunt resistance of the **non-UV-ZnO device** (i.e. slope at the Jsc region). However, with UV ozone treatment, the work function of the **UV-ZnO** device is increased to 5.2 eV. The large work function difference between electrodes leads to a strong built-in field. This can drive the free holes and electrons towards the electrodes and prevent the undesired charge recombination.

The dark current densities of these devices are also shown in Fig. 1d. The dark current of the **UV-ZnO device** is much smaller than that of **non-UV-ZnO device**. Its leakage current density under -1.5 V bias is at 10^{-4} mA/cm^2, which is 10 times smaller than that of the standard **UV-ITO device** (10^{-3} mA/cm^2). This explained why the Voc of the **UV-ZnO device** is the highest (1.06 V) among the three devices. [38]

To understand the photoresponse of the above devices, the external quantum efficiencies (EQE) of **UV-ITO** and **UV-ZnO devices** are examined with results shown in Fig. 2a. The EQE peaks observed at 350 and 590 nm correspond to the photo-absorption of C_{60} and SubPc, respectively. In Fig. 2a, while the EQE signal of two devices at the C_{60} response range (350 nm) are similar; the EQE signal of **UV-ZnO device** at 590 nm (i.e. SubPc photoresponse) is ~10 % higher than that of the **UV-ITO device**. Fig. 2b shows the absorption of 10 nm SubPc (peaked at 590 nm) prepared on **UV-ITO** and **UV-ZnO** substrates. The improved absorption after introducing ZnO layer is consistent with the EQE enhancement.

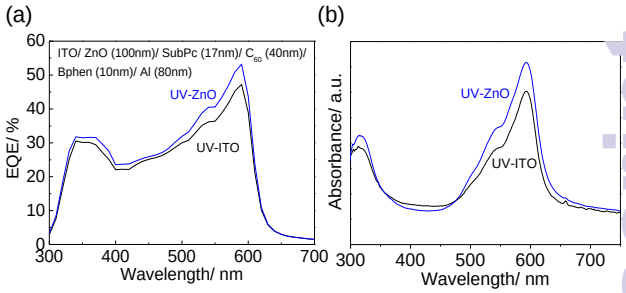

Fig. 2(a) External quantum efficiency (EQE) spectra of standard UV-ITO and UV-ZnO devices. (b) Absorption spectra of 10 nm SubPc prepared on UV-ITO and UV-ZnO substrates.

To understand the SubPc absorption enhancement, the surface morphologies of the **UV-ITO and UV-ZnO** substrates are studied with results shown in Fig. 3a-b. The root mean square (r.m.s) roughness of a **UV-ZnO** substrate is 3.65 nm, which is much high than the **UV-ITO** substrate (i.e 0.66 nm). More interestingly, the ZnO roughness is found to have a close relationship with the device Jsc as shown in Fig. 3c. The AFM results suggest that absorption enhancement in SubPc might attribute to light scattering at ZnO/ SubPc surface, which in turn leads to the Jsc improvement[39].

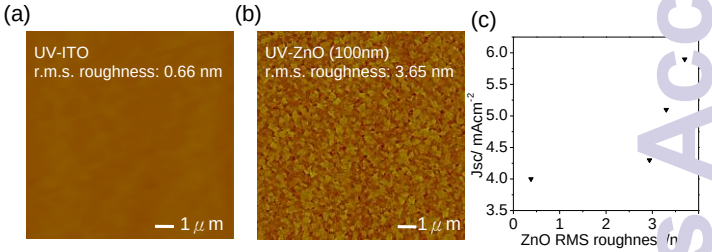

Fig 3. AFM images showing the r.m.s. roughness of (a) ITO and (b) UV-ZnO substrates. (c) The relationship between the Jsc and the ZnO r.m.s. roughness.

We continue the discussion by examining the operation stabilities of **UV-ITO** and **UV-ZnO devices.** Fig. 4a-d compare degradation rates of the two devices measured under continuous AM 1.5G 1 Sun illumination for 60 minutes. The photovoltaic parameters are normalized for better comparison. Along with timed illumination, the PCE of the standard **UV-ITO device** gradually degrades in 60 minutes. Noteworthy, by introducing ZnO layer (**UV-ZnO devices**), the drop of PCE is significantly suppressed. More importantly, a very high Voc of >1 V is maintained in this device throughout the test (Fig. 4b). The changes in Jsc (Fig. 4c) and FF (Fig. 4d) are much smaller than that in Voc (Fig. 4b).

Fig. 4e shows the dark current density of both **UV-ITO** and **UV-ZnO** devices before and after 60 minutes operation. The onset of the dark J-V curve for the **UV-ITO** device is decreased from 0.78 V to 0.68 V after operation, suggesting a decrease in built-in voltage after operation. However, the dark J-V curve of **UV-ZnO** device has only limited change, implying the device have limited change in built in voltage, and thus is more stable. To consolidate our discussion, we carried out UPS studies on the **UV-ITO and UV-ZnO** substrates. Fig. 4f compares cutoff positions of the UPS spectra of **UV-ITO** and **UV-ZnO** samples before and after time storage in ultrahigh vacuum (UHV) condition. The bottom spectra show the UV ozone treated fresh substrates. After one day storage, the cut-off position of **UV-ITO** substrate shifted to the higher binding energy region by 0.21 eV, indicating the work function decreases after storage. However, the spectral cut-off shift in **UV-ZnO** is only 0.13 eV. The stable work function of **UV-ZnO** substrate explains the enhanced device stability of **UV-ZnO device**.

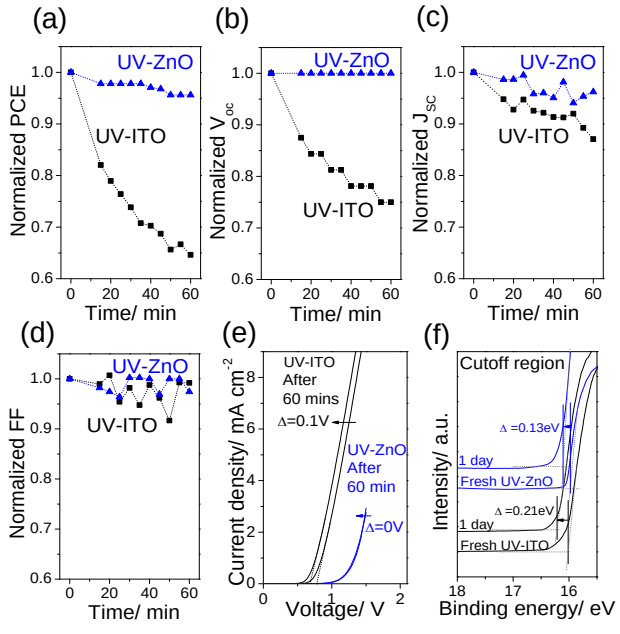

Fig 4. Normalized (a) PCE (b) Voc (c) Jsc and (d) FF of UV-ITO and UV-ZnO (100 nm) device for 60 min illumination. (e) The dark J-V curves before and after the stability test of both devices. (f) The UPS spectra of UV-ITO and UV-ZnO (100 nm) after storage for one day in ultrahigh vacuum condition

Conclusions

In conclusion, we demonstrated the performance of solar cell can be improved by using ITO/ZnO anode with post UV ozone treatment. The device with UV ozone treated ITO/ZnO substrate has higher Jsc and Voc compared to that with standard UV-ITO substrate. PCE up to 3.2% has been achieved with good device stability. The enhancements were shown to be due to the higher work function of ITO/ZnO substrate after UV ozone treatment. And also, the improved SubPc absorption is due to light scattering of ITO/ZnO surface. More importantly, the **UV-ZnO** has device stability under continuous illumination for 60 minutes.

Acknowledgements

The work described in this paper was supported by a grant from the Research Grants Council of the Hong Kong Special Administrative Region, China (Project No. T23–713/11); and National Natural Science Foundation of China (No. 21303150).

References

1. S. R. Forrest, *Nature*, 2004, **428**, 911-918.
2. X. Tong, N. Wang, M. Slootsky, J. Yu and S. R. Forrest, *Solar Energy Materials and Solar Cells*, 2013, **118**, 116-123.
3. N. Wang, X. Tong, Q. Burlingame, J. Yu and S. R. Forrest, *Solar Energy Materials and Solar Cells*, 2014, **125**, 170-175.
4. M. Manceau, E. Bundgaard, J. E. Carlé, O. Hagemann, M. Helgesen, R. Søndergaard, M. Jørgensen and F. C. Krebs, *Journal of Materials Chemistry*, 2011, **21**, 4132-4141.
5. Y. H. Kim, C. Sachse, M. Hermenau, K. Fehse, M. Riede, L. Müller-Meskamp and K. Leo, *Applied Physics Letters*, 2011, **99**, 113305.
6. R. Lessmann, Z. Hong, S. Scholz, B. Maennig, M. Riede and K. Leo, *Organic Electronics*, 2010, **11**, 539-543.
7. A. Rivaton, S. Chambon, M. Manceau, J.-L. Gardette, N. Lemaître and S. Guillerez, *Polymer Degradation and Stability*, 2010, **95**, 278-284.
8. F. C. Krebs and K. Norrman, *Progress in Photovoltaics: Research and Applications*, 2007, **15**, 697-712.
9. M. O. Reese, A. M. Nardes, B. L. Rupert, R. E. Larsen, D. C. Olson, M. T. Lloyd, S. E. Shaheen, D. S. Ginley, G. Rumbles and N. Kopidakis, *Advanced Functional Materials*, 2010, **20**, 3476-3483.
10. M. Jørgensen, K. Norrman and F. C. Krebs, *Solar Energy Materials and Solar Cells*, 2008, **92**, 686-714.
11. S. Schäfer, A. Petersen, T. A. Wagner, R. Kniprath, D. Lingenfelser, A. Zen, T. Kirchartz, B. Zimmermann, U. Würfel and X. Feng, *Physical Review B*, 2011, **83**, 165311.

12. M. F. Lo, T. W. Ng, H. W. Mo and C. S. Lee, *Advanced Functional Materials*, 2013, **23**, 1718-1723.
13. X. Cao and Y. Zhang, *Applied Physics Letters*, 2012, **100**, 183304.
14. M. F. Lo, T. W. Ng, S. Lai, M. K. Fung, S. T. Lee and C. S. Lee, *Applied Physics Letters*, 2011, **99**, 033302.
15. J. Tang, Y. Li, L. Hung and C. Lee, *Applied Physics Letters*, 2004, **84**, 73-75.
16. Q.-D. Yang, T.-W. Ng, M.-F. Lo, N.-B. Wong and C.-S. Lee, *Organic Electronics*, 2012, **13**, 3220-3225.
17. H. P. Kim, A. R. bin Mohd Yusoff and J. Jang, *Solar Energy Materials and Solar Cells*, 2013, **110**, 87-93.
18. Y. Gao, H.-L. Yip, S. K. Hau, K. M. O'Malley, N. C. Cho, H. Chen and A. K.-Y. Jen, *Applied Physics Letters*, 2010, **97**, 203306.
19. T. Dobbertin, O. Werner, J. Meyer, A. Kammoun, D. Schneider, T. Riedl, E. Becker, H.-H. Johannes and W. Kowalsky, *Applied Physics Letters*, 2003, **83**, 5071-5073.
20. W.-T. Chiang, S.-H. Su, Y.-F. Lin and M. Yokoyama, *Japanese Journal of Applied Physics*, 2010, **49**, 04DK14.
21. X. Fan, C. Cui, G. Fang, J. Wang, S. Li, F. Cheng, H. Long and Y. Li, *Advanced Functional Materials*, 2012, **22**, 585-590.
22. F. Wang, G. Sun, C. Li, J. Liu, S. Hu, H. Zheng, Z. a. Tan and Y. Li, *ACS applied materials & interfaces*, 2014, **6**, 9458-9465.
23. E. L. Ratcliff, J. Meyer, K. X. Steirer, A. Garcia, J. J. Berry, D. S. Ginley, D. C. Olson, A. Kahn and N. R. Armstrong, *Chemistry of Materials*, 2011, **23**, 4988-5000.
24. Q. Xu, F. Wang, Z. a. Tan, L. Li, S. Li, X. Hou, G. Sun, X. Tu, J. Hou and Y. Li, *ACS applied materials & interfaces*, 2013, **5**, 10658-10664.
25. D.-J. Yun, H.-m. Ra, S. B. Jo, W. Maeng, S.-h. Lee, S. Park, J.-W. Jang, K. Cho and S.-W. Rhee, *ACS applied materials & interfaces*, 2012, **4**, 4588-4594.
26. J. Luo, L. Xiao, Z. Chen, B. Qu and Q. Gong, *Journal of Physics D: Applied Physics*, 2010, **43**, 385101.
27. V. Shrotriya, G. Li, Y. Yao, C.-W. Chu and Y. Yang, *Applied Physics Letters*, 2006, **88**, 073508.
28. H. Wang, Z. Liu, M. F. Lo, T. W. Ng, D. Yan and C.-S. Lee, *Applied Physics Letters*, 2012, **100**, 103302.
29. S. Tokito, K. Noda and Y. Taga, *Journal of Physics D: Applied Physics*, 1996, **29**, 2750.
30. M. D. Irwin, D. B. Buchholz, A. W. Hains, R. P. Chang and T. J. Marks, *Proceedings of the National Academy of Sciences*, 2008, **105**, 2783-2787.
31. Y.-H. Kim, S.-H. Lee, J. Noh and S.-H. Han, *Thin Solid Films*, 2006, **510**, 305-310.
32. M. Zhang, H. Ding, Y. Gao and C. Tang, *Applied Physics Letters*, 2010, **96**, 183301.
33. M. Vasilopoulou, A. M. Douvas, D. G. Georgiadou, L. C. Palilis, S. Kennou, L. Sygellou, A. Soultati, I. Kostis, G. Papadimitropoulos and D. Davazoglou, *Journal of the American Chemical Society*, 2012, **134**, 16178-16187.
34. M. White, D. Olson, S. Shaheen, N. Kopidakis and D. S. Ginley, *Applied Physics Letters*, 2006, **89**, 143517.
35. J.-C. Wang, W.-T. Weng, M.-Y. Tsai, M.-K. Lee, S.-F. Horng, T.-P. Perng, C.-C. Kei, C.-C. Yu and H.-F. Meng, *Journal of Materials Chemistry*, 2010, **20**, 862-866.
36. S. Schumann, R. Da Campo, B. Illy, A. Cruickshank, M. McLachlan, M. Ryan, D. Riley, D. McComb and T. S. Jones, *Journal of Materials Chemistry*, 2011, **21**, 2381-2386.
37. T. W. Ng, M. F. Lo, Q. D. Yang, M. K. Fung and C. S. Lee, *Advanced Functional Materials*, 2012, **22**, 3035-3042.
38. B. P. Rand, D. P. Burk and S. R. Forrest, *Physical Review B*, 2007, **75**, 115327.
39. Z. Hu, J. Zhang, Y. Liu, Y. Li, X. Zhang and Y. Zhao, *Synthetic Metals*, 2011, **161**, 2174-2178.

A table of contents entry:

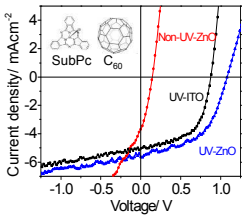

Improved PCE (from 2.5 to 3.2 %) and stability of SubPc/C_{60}-based OPV device using an UV-ozone treated ZnO anode buffer.